

RESPONSE SURFACE OPTIMIZATION OF FLUIDIZED ROASTING REDUCTION OF LOW-GRADE PYROLUSITE COUPLING WITH PRETREATMENT OF STONE COAL

Y. Feng ^a, Z. Cai ^a, H. Li ^b, Z. Du ^b, X. Liu ^{a,*}

^a School of Civil and Environmental Engineering, University of Science and
Technology Beijing, Beijing, China;

^b State Key Laboratory of Biochemical Engineering, Institute of Process
Engineering, Chinese Academy of Sciences, Beijing, China

(Received 25 May 2012; accepted 18 October 2012)

Abstract

Research on the novel technology of fluidized roasting reduction of low-grade pyrolusite coupling with pretreatment of stone coal has been conducted. According to the response surface design and the analysis of results, orthogonal experiments have been conducted on the major factors and effects of the factors on the manganese reduction efficiency have been studied. The quadratic model between the manganese reduction efficiency and the factors has been established. Meanwhile, the contour or 3D response surface of the manganese reduction efficiency among various factors has been presented. The maximum manganese reduction efficiency could be optimized to nearly 100 %, when the mass ratio of stone coal to pyrolusite was 2.5:1, the roasting temperature of stone coal was 1080 °C, the roasting temperature of pyrolusite was 775 °C, and the roasting time was 2 h. The results of the manganese reduction efficiency of the actual experiments were close to those of the fitting model by the verification experiments, indicating that the optimum solution has a relatively high reliability. Other low-grade pyrolusite such as Guangxi pyrolusite (China), Hunan pyrolusite (China), and Guizhou pyrolusite (China) were tested and all these materials responded well giving nearly 100 % manganese reduction efficiency.

Keywords: *Response surface optimization; Fluidized roasting; Coupling technology; Low-grade pyrolusite reduction; Stone coal pretreatment*

1. Introduction

Manganese is one of the significant strategic resources that plays important roles in many fields, such as ferrous metallurgy, nonferrous metal production, battery production, and fine chemicals [1, 2]. With the ever increasing demand for manganese resources and the shortage of high grade ores, exploitation and utilization of low-grade manganese ores become urgent [3]. Manganese presents in the form of MnO₂ in pyrolusite. As manganese dioxide ores are stable in acidic or alkali oxidizing conditions, the extraction for manganese in pyrolusite must be carried out in reductive conditions to obtain acid-soluble manganese oxide [4]. There are two kinds of reductive technologies for pyrolusite at present: the roasting reduction and the hydrometallurgical reduction. The roasting reduction can be held in a reverberating furnace, a rotary kiln or a fixed bed

using CO [5] or H₂ [6, 7] as the reductive gas or organic materials as the reductants such as cornstalk [8], and sawdust [9] at high temperature. The process has many disadvantages: high energy consumption, long roasting time, insufficient heat and mass transfer, and easy sintering. The hydrometallurgical reduction proceeds mainly with the following reductants: reductive minerals, including pyrite [10], sphalerite [11], and galena [12]; organic reductive materials, including molasses [2, 13], methyl alcohol [14, 15], sawdust [16], cornstalk [17], and oxalic acid [4]; and inorganic reductants, including sodium sulfite [18], iron powder [19], ferrous sulphate [20], hydrogen peroxide [21-23], and sulfur dioxide [24-26].

Stone coal, mainly consisting of silicate minerals, contains a small amount of carbon components. Vanadium resources in China primarily exist in stone coal and its V₂O₅ reserves accounts for more than 85% of the total reserves nationwide [27]. Therefore, stone

* Corresponding author: 2501193438@qq.com

coal is essential to vanadium extraction. During its vanadium extracting process, hydrophobicity of the stone coal surface formed by the carbon components may hinder the acid or alkaline leaching agents from contacting with the vanadium, thus causing low vanadium extracting efficiency. Therefore, stone coal should be usually pretreated by oxidizing roasting to remove the carbon components before the vanadium extraction.

In this paper, a novel technology, that is to couple the pretreatment of stone coal with the roasting reduction process of low-grade pyrolusite, was presented. In order to make full use of the carbon components in stone coal, it was used as the reductant in low-grade pyrolusite processing. This eco-friendly coupling mine processing technology can not only maximize the utilization of stone coal and benefit the following step of the vanadium extraction, but also decrease the emission of harmful gases such as CO and SO₂ during the oxidizing roasting pretreatment of stone coal for the vanadium extraction. At the same time, fluidized roasting, which was characterized by large phase contact area, sufficient heat and mass transfer, not easy sintering, and high reaction rate and efficiency, was adopted in the whole process, i.e. in both the pretreatment roasting stage of stone coal and the reductive roasting of pyrolusite. Therefore, the novel fluidized roasting coupling technology could achieve the goal of the efficient exploitation.

2. Materials and methods

2.1. Materials

The sample of stone coal was obtained from Guangxi, China. The ore sample was crushed and ground into powder with the particle size smaller than 0.074 mm. The chemical multi-elemental analysis showed that the stone coal used contained 6.72 % Al, 23.88 % Si, and 17.75 % C as listed in Table 1. The mineralogical composition of the ore sample was defined by powder X-ray diffraction. The XRD pattern (Figure 1) showed that the main minerals included quartz, muscovite, and phlogopite.

Table 1. The chemical multi-elemental analysis of stone coal / %

V	Al	Si	C	S	Ca	Mg	Fe
0.62	6.72	23.88	17.75	2.25	3.44	5.58	0.11

The sample of low-grade pyrolusite was obtained from Yunnan, China. The ore sample was crushed and ground into powder with the particle size smaller than

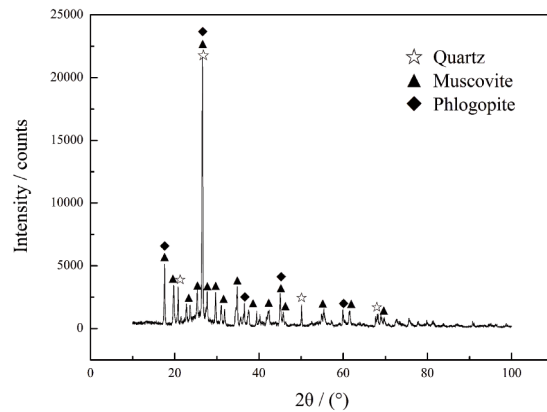


Figure 1. The XRD image of stone coal

0.147 mm. The chemical multi-elemental analysis (as listed in Table 2) showed that the pyrolusite used contained 21.43 % Mn, 36.36 % SiO₂, and 8.11 % Fe₂O₃. Powder X-ray diffraction (Figure 2) showed that manganese was mainly in the form of manganese dioxide in pyrolusite, and the main gangue minerals included quartz and feldspar.

Table 2. The chemical multi-elemental analysis of low-grade pyrolusite / %

Mn	SiO ₂	Fe ₂ O ₃	Al ₂ O ₃	CaO	Na ₂ O	MgO	S	P
21.43	36.36	8.11	7.79	5.31	2.79	1.93	0.2	0.02

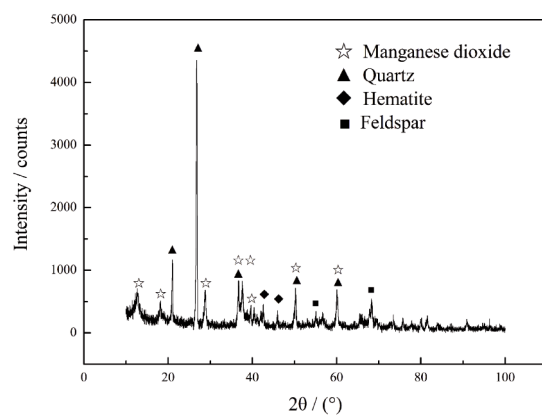


Figure 2. The XRD image of low-grade pyrolusite

2.2. Experimental equipment

Figure 3 showed the experimental equipment designed by ourselves. It consisted of two quartz fluidized bed reactors, nitrogen cylinder, rotameter, steam generator, crucible resistance furnace, and acidometer. The nitrogen used in the experiment was industrial grade. All other chemicals were of

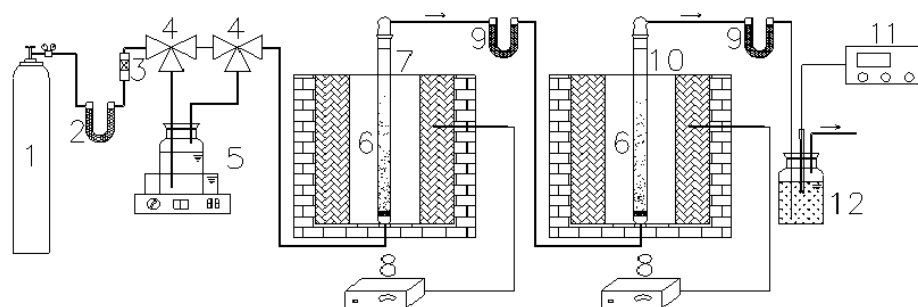


Figure 3. The Schematic diagram of fluidized roasting coupling reactor (1 nitrogen cylinder; 2 dryer; 3 rotameter; 4 three-way valve; 5 steam generator; 6 crucible resistance furnace; 7 quartz fluidized bed reactor I (stone coal); 8 electronic thermo-controllers; 9 absorber; 10 quartz fluidized bed reactor II (low-grade pyrolusite); 11 acidometer; 12 alkali liquor bottle)

analytical grade and used without further purification. Calcium chloride anhydrous was used as absorber. The first absorber after the quartz fluidized bed reactor I was used to dry the reductive gas mixture (CO and H₂) so that the manganese in low-grade pyrolusite could be reduced more effectively. The second absorber after quartz fluidized bed reactor II was used to absorb the steam generated from the manganese reduction reaction by H₂ and the increase weight of absorber could provide some guidance for the material balance calculation of the whole system to some extent.

2.3. Experimental procedure

Fluidized gas flow rate required for suspending ore powder in roasting was determined by cold gas flow experiment according to the flow characteristic curve of the pressure drop of feed layer. The results indicated that the preferable flow rate of steam was 0.4 m³/h.

After crushing, rod milling, screening, and drying, 10 g of stone coal and a certain amount of pyrolusite were added into the quartz fluidized bed reactor I and II, respectively according to the mass ratio of stone coal to pyrolusite. Then N₂ was introduced into the reactors to remove the oxidizing atmosphere. When both stone coal and pyrolusite were roasted at the designated temperature, the three-way valve was switched to let N₂ feed into the steam generator at 80 °C so as to load steam into the fluidized bed reactor I to react with the carbon components in stone coal to produce CO and H₂. The reductive gas mixture was then fed into the fluidized bed reactor II to reduce the manganese in low-grade pyrolusite. After the roasting reduction completed, the roasted product was put into a leaching pod containing enough quantities of

sulphuric acid immediately lest the reduced ore was reoxidized by oxygen of air. The solution was stirred continuously until all the manganese oxide was leached from the roasting product. After the sample was filtrated and dried, manganese in filtrate was analyzed to calculate the manganese leaching efficiency and it can be indicated by manganese reduction efficiency, due to the fact that manganese dioxide can not be dissolved by sulphuric acid. The composition of gases in reactor I during roasting was H₂, CO, N₂, and a small amount of H₂O (g). The main chemical reaction related in reactor I was shown in chemical equation (1) as follows. The composition of gases in reactor II during roasting was H₂O (g), CO₂, and N₂. The main chemical reactions related in reactor II were shown in chemical equation (2) and (3) as follows.



3. Results and discussion

3.1. Response surface analysis and experimental optimization

3.1.1. Factors and levels selection

The primary impact factors of the manganese reduction efficiency include the mass ratio of stone coal to pyrolusite, the roasting temperature of stone coal, the roasting temperature of pyrolusite, and roasting time. In order to obtain a relatively high manganese reduction efficiency, the conditions of the single factors should be: the mass ratio of stone coal to pyrolusite, 3:1; the roasting temperature of stone

coal, 1000 °C; the roasting temperature of pyrolusite, 800 °C; and the roasting time, 2 h; respectively, according to the single factor experiments. Based on the results above, the appropriate boundary value of every factor has been determined to proceed to the Box-Behnken orthogonal experiments of four factors and three levels (Table 3).

3.1.2. Experimental results and analysis

The results of orthogonal experiments are shown in Table 4. Sum of squares and summary statistics of various fitting models between the manganese reduction efficiency and every factor are listed in Table 5 and Table 6, respectively.

Linear, two-factor interaction (2FI), quadratic, and cubic polynomials were fitted to the response. Table 5 shows how terms of increasing complexity contribute

Table 3. The factors and levels of orthogonal experiments

Factor	Name	Units	Coded Level Values		
			-1	0	1
A	The mass ratio of stone coal to pyrolusite	—	2	3	4
B	The roasting temperature of stone coal	°C	900	1000	1100
C	The roasting temperature of pyrolusite	°C	750	800	850
D	Roasting time	h	1.5	2	2.5

to the total model. The model hierarchy is described below:

“Linear vs Mean”: the significance of adding the linear terms to the mean,

“2FI vs Linear”: the significance of adding the two factor interaction terms to the mean and linear terms

Table 4. The results of orthogonal experiments for Box-Behnken design

No.	A The mass ratio of stone coal to pyrolusite	B The roasting temperature of stone coal / °C	C The roasting temperature of pyrolusite / °C	D Roasting time / h	Manganese reduction efficiency / %
1	1	0	1	0	97.98
2	0	-1	0	1	58.54
3	-1	-1	0	0	41.31
4	0	-1	1	0	59.86
5	1	-1	0	0	66.45
6	0	1	-1	0	93.42
7	1	0	-1	0	95.17
8	0	0	1	1	95.94
9	0	1	0	1	99.11
10	1	1	0	0	99.16
11	0	0	1	-1	90.05
12	-1	1	0	0	97.53
13	1	0	0	-1	92.23
14	-1	0	-1	0	78.35
15	0	0	0	0	98.93
16	0	1	1	0	98.84
17	1	0	0	1	99.35
18	0	-1	0	-1	38.72
19	0	0	0	0	98.96
20	-1	0	1	0	91.19
21	0	0	-1	-1	72.67
22	0	0	0	0	98.89
23	-1	0	0	-1	75.52
24	0	0	-1	1	95.77
25	0	1	0	-1	89.98
26	0	-1	-1	0	45.82
27	0	0	0	0	98.94
28	-1	0	0	1	96.11
29	0	0	0	0	98.98

Table 5. Sequential model sum of squares for Box-Behnken design

Source	Sum of Squares	df	Mean Square	F Value	p-value Prob>F	
Mean vs Total	2.09E+05	1	2.09E+05			
Linear vs Mean	7210.5	4	1802.62	13.93	<0.0001	
2FI vs Linear	329.88	6	54.98	0.36	0.8968	
Quadratic vs 2FI	2754.44	4	688.61	443.73	<0.0001	Suggested
Cubic vs Quadratic	11.36	8	1.42	0.82	0.6123	Aliased
Residual	10.36	6	1.73			
Total	2.20E+05	29	7573.53			

Table 6. Model summary statistics for Box-Behnken design

Source	Std. Dev.	R- Squared	Adjusted R- Squared	Predicted R- Squared	PRESS	
Linear	11.38	0.6989	0.6487	0.5751	4383.98	
2FI	12.42	0.7309	0.5814	0.3196	7019.4	
Quadratic	1.25	0.9979	0.9958	0.9879	125.12	Suggested
Cubic	1.31	0.999	0.9953	0.8554	1491.79	Aliased

already in the model,

“Quadratic vs 2FI”: the significance of adding the quadratic (squared) terms to the mean, linear, and two-factor interaction terms already in the model,

“Cubic vs Quadratic”: the significance of the cubic terms beyond all other terms.

For each source of terms (linear, etc.), the probability value (“Prob > F”) should be examined to see if it falls below 0.05. The extremely low p-value indicates a highly significant advantage when adding this level to what’s already been built.

The results indicated that the fitting model of quadratic was relatively great and suggested. The F value of the quadratic fitting model was 443.73, and the p value was smaller than 0.0001, indicating that this model had statistical significance.

Table 6 shows that the quadratic model comes out best, because of its lower Std. Dev. (standard deviation) and better R-squared values – raw, adjusted, and predicted compared with lower-order models. Also the quadratic model produces the least PRESS (predicted residual sum of squares) – a good measure of its relative precision for forecasting future outcomes.

The quadratic model fitted well with the experimental results and using this model for fitting actual experiments was feasible.

The confidence degree analysis of quadratic model is shown in Table 7. The model coefficients include confidence intervals (CI) and the variance

inflation factors (VIF) – a measure of factor collinearity. A value of 1 is ideal (orthogonal), but a VIF below 10 is generally accepted. A VIF above 1000 indicates severe multicollinearity in the model coefficients.

The results indicated that the fitting results of quadratic model were significant. The impact sequence of single factors to the manganese reduction efficiency is shown as: the roasting temperature of stone coal > roasting time > the mass ratio of stone coal to pyrolusite > the roasting temperature of pyrolusite. The impact sequence of interaction factors to the manganese reduction efficiency is presented as: (the mass ratio of stone coal to pyrolusite × the roasting temperature of stone coal) > (the roasting temperature of pyrolusite × roasting time) > (the mass ratio of stone coal to pyrolusite × roasting time) > (the roasting temperature of stone coal × roasting time) > (the mass ratio of stone coal to pyrolusite × the roasting temperature of pyrolusite) > (the roasting temperature of stone coal × the roasting temperature of pyrolusite).

The quadratic model between the manganese reduction efficiency and every factor could be expressed as follows:

$$\begin{aligned} \eta = & 98.94 + 5.86A + 22.28B + 4.39C + 7.14D \\ & - 5.88AB - 2.51AC - 3.37AD - 2.15BC - 2.67BD \\ & - 4.30CD - 2.72A^2 - 20.42B^2 - 4.63C^2 - 6.02D^2 \end{aligned}$$

Normal plot of residuals is shown in Figure 4. The

Table 7. The confidence degree analysis of quadratic model

Factor	Coefficient Estimate	df	Standard Error	95% CI Low	95% CI High	VIF
Intercept	98.94	1	0.56	97.75	100.13	
A- The mass ratio of stone coal to pyrolusite	5.86	1	0.36	5.09	6.63	1
B- The roasting temperature of stone coal	22.28	1	0.36	21.51	23.05	1
C- The roasting temperature of pyrolusite	4.39	1	0.36	3.62	5.16	1
D- Roasting time	7.14	1	0.36	6.37	7.91	1
AB	-5.88	1	0.62	-7.21	-4.54	1
AC	-2.51	1	0.62	-3.84	-1.17	1
AD	-3.37	1	0.62	-4.7	-2.03	1
BC	-2.15	1	0.62	-3.49	-0.82	1
BD	-2.67	1	0.62	-4.01	-1.34	1
CD	-4.3	1	0.62	-5.64	-2.97	1
A ²	-2.72	1	0.49	-3.77	-1.67	1.08
B ²	-20.42	1	0.49	-21.47	-19.37	1.08
C ²	-4.63	1	0.49	-5.68	-3.58	1.08
D ²	-6.02	1	0.49	-7.06	-4.97	1.08

points were almost distributed in a line, indicating that the model fitted relatively well.

Contours between the mass ratio of stone coal to pyrolusite and the roasting temperature of stone coal for the manganese reduction efficiency are shown in Figure 5, under the conditions that the roasting temperature of pyrolusite was 800 °C and the roasting time was 2 h. The results indicated that the roasting temperature of stone coal should be gradually reduced with the increase of the mass ratio of stone coal to pyrolusite when the manganese reduction efficiency was 86.2281 % and the conditions of the roasting temperature of pyrolusite and the roasting time were intermediate level.

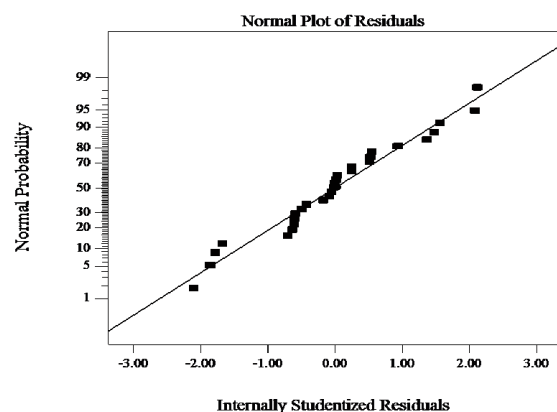
Contours between the mass ratio of stone coal to pyrolusite and the roasting time for the manganese reduction efficiency are shown in Figure 6, with fixing the roasting temperature of stone coal at 1000 °C and the roasting temperature of pyrolusite at 800 °C. The results indicated that the roasting time should be gradually reduced with the increase of the mass ratio of stone coal to pyrolusite when the manganese reduction efficiency was 75.5834 % and the roasting temperature of stone coal and the roasting temperature of pyrolusite were intermediate level.

Response surface between the roasting temperature of pyrolusite and the roasting time for the manganese reduction efficiency is shown in Figure 7, while fixing the mass ratio of stone coal to pyrolusite at 3:1 and the roasting temperature of stone coal at 1000 °C. The manganese reduction efficiency

increased with the increase of the roasting temperature of pyrolusite when the conditions of the mass ratio of stone coal to pyrolusite and the roasting temperature of stone coal were intermediate level. The manganese reduction efficiency increased with the extension of the roasting time. When the roasting time was 2 h, the manganese reduction efficiency was maximized, which agreed with the results of the single factor experiments.

3.1.3. Experimental optimization

Based on the experimental results and the fitting model analysis, the optimization for the level of every factor could be conducted on the basis of the maximum manganese reduction efficiency (Table 8). When the

**Figure 4.** Normal plot of residuals

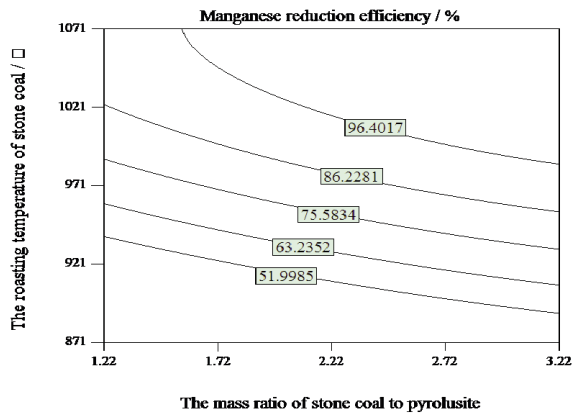


Figure 5. Contours between the mass ratio of stone coal to pyrolusite and the roasting temperature of stone coal for the manganese reduction efficiency

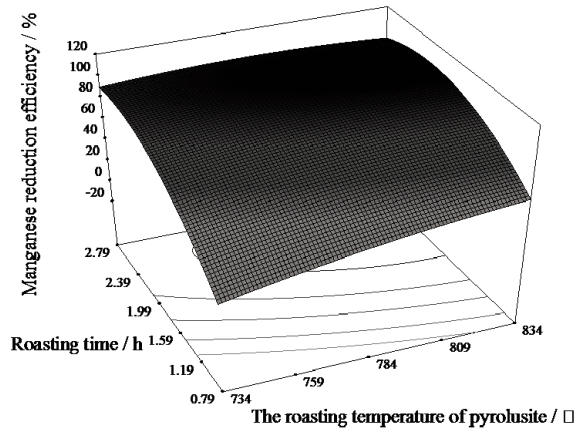


Figure 7. Response surface between the roasting temperature of pyrolusite and roasting time for the manganese reduction efficiency

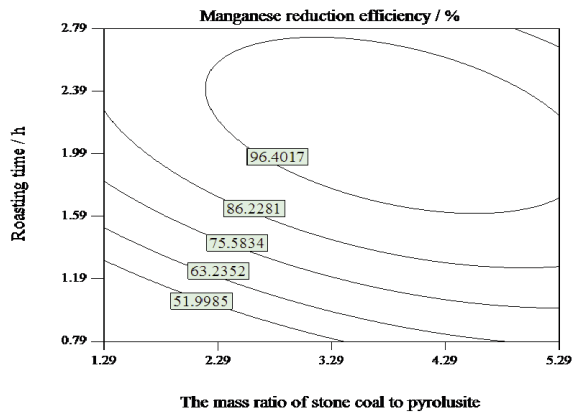


Figure 6. Contours between the mass ratio of stone coal to pyrolusite and roasting time for the manganese reduction efficiency

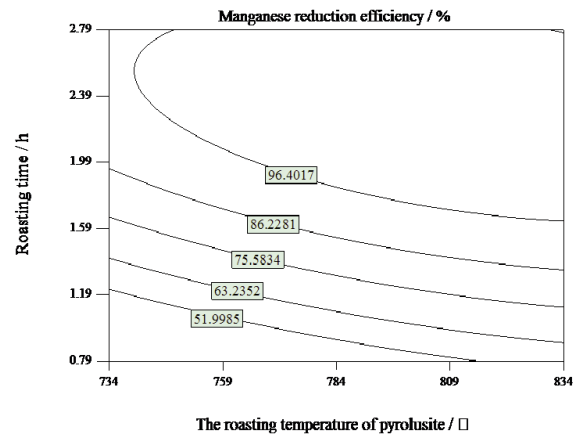


Figure 8. Optimized contours between the roasting temperature of pyrolusite and roasting time for the manganese reduction efficiency

mass ratio of stone coal to pyrolusite was 2.5:1, the roasting temperature of stone coal was 1080 °C, the roasting temperature of pyrolusite was 775 °C, and the roasting time was 2 h, the maximum manganese reduction efficiency, nearly 100 %, could be obtained. The optimized contours and response surface between the roasting temperature of pyrolusite and the roasting time for the manganese reduction efficiency of the No. 1 optimization scheme are shown in Figure 8 and Figure 9, respectively, under the conditions that the mass ratio of stone coal to pyrolusite was 2.5:1, and the roasting temperature of stone coal was 1080 °C. Three verification experiments were conducted according to the No. 1 optimization scheme and the results of the manganese reduction efficiency were 99.91 %, 100.00 %, and 99.97 %, respectively, which were close to the results of the fitting model, indicating that the optimum solution had a relatively high reliability.

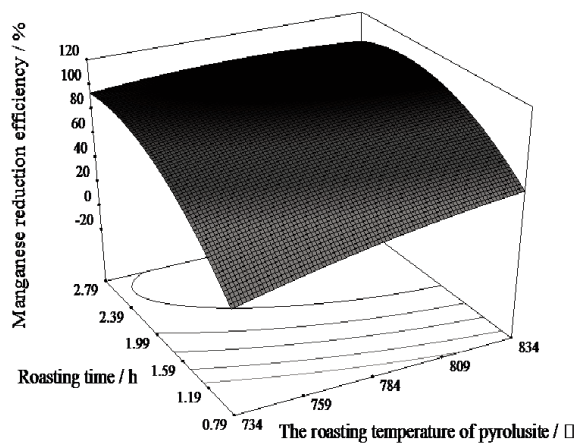


Figure 9. Optimized response surface between the roasting temperature of pyrolusite and roasting time for the manganese reduction efficiency

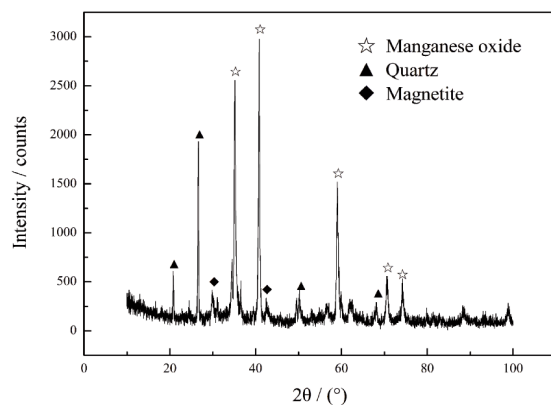
Table 8. Optimization scheme of the experiments

No.	The mass ratio of stone coal to pyrolusite	The roasting temperature of stone coal / °C	The roasting temperature of pyrolusite / °C	Roasting time / h	Manganese reduction efficiency / %	Desirability
1	2.5	1080	775	2	100.166	1
2	3.94	1050	800	1.65	100.319	1
3	3.16	1025	810	2.15	105.303	1
4	3.77	1080	800	2	103.016	1
5	3.85	1015	795	2.45	103.161	1
6	3.85	1015	845	2	102.304	1
7	3.1	1010	805	2	102.36	1
8	2.2	1045	780	2.5	101.944	1
9	2.85	1080	800	2.4	104.39	1
10	2.3	1060	835	2	102.922	1

Table 9. Reduction behaviour of other low-grade pyrolusite

Roasting time	Manganese reduction efficiency / %					Condition (Stone coal)
	0.5 h	1 h	1.5 h	2 h	2.5 h	
Guangxi pyrolusite (Mn 26.09 %)	65.63	80.77	92.25	99.96	99.98	30 g
Hunan pyrolusite (Mn 17.78 %)	60.44	74.35	87.72	99.92	99.95	22 g
Guizhou pyrolusite (Mn 21.36 %)	59.09	76.57	89.48	100	99.97	25 g

The XRD image of the roasting product of pyrolusite under the No. 1 optimization scheme is shown in Figure 10. The main minerals included manganese oxide, quartz, and a small amount of magnetite. The diffraction peak of MnO_2 was basically vanished but the diffraction peak of MnO appeared and increased clearly. The fact that the maximum manganese reduction efficiency of pyrolusite under this condition could be obtained has been further confirmed.

**Figure 10.** The XRD image of the fluidized roasting reductive product of pyrolusite under the No. 1 optimization scheme

3.2. Reduction behaviour of other low-grade pyrolusite

Other low-grade pyrolusite such as Guangxi pyrolusite (China), Hunan pyrolusite (China), and Guizhou pyrolusite (China) were tested at ore sample 10 g, the roasting temperature of stone coal 1080 °C, the roasting temperature of pyrolusite 775 °C, and the results are shown in Table 9. The amount of stone coal for these materials was varied to optimize the manganese reduction efficiency. The amounts corresponding to maximum reduction efficiency showed that the amount of the required stone coal was dependant on the manganese content of pyrolusite and the requirement decreased with the decrease in Mn content. The present study established the suitability of stone coal as reductant for various low-grade pyrolusite.

4. Conclusions

(1) The novel technology of fluidized roasting reduction of low-grade pyrolusite coupling with pretreatment of stone coal for the manganese exploitation and utilization is green and eco-friendly, because it can not only maximize the utilization of stone coal and benefit the following step of the

vanadium extraction, but also decrease the emission of harmful gases such as CO and SO₂ during the oxidizing roasting pretreatment of stone coal for the vanadium extraction.

(2) Based on the primary factors and levels determined by the single factor experiments, the design, analysis, and optimization of the orthogonal experiments have been conducted. The results indicated that the most effective single factor for the manganese reduction efficiency was the roasting temperature of stone coal, and the most effective interaction factor for the manganese reduction efficiency was (the mass ratio of stone coal to pyrolusite × the roasting temperature of stone coal). The quadratic model between the manganese reduction efficiency and every factor could be expressed as follows:

$$\begin{aligned} \eta = & 98.94 + 5.86A + 22.28B + 4.39C + 7.14D \\ & - 5.88AB - 2.51AC - 3.37AD - 2.15BC - 2.67BD \\ & - 4.30CD - 2.72A^2 - 20.42B^2 - 4.63C^2 - 6.02D^2 \end{aligned}$$

(3) According to the optimization scheme of the experiments, when the mass ratio of stone coal to pyrolusite was 2.5:1, the roasting temperature of stone coal was 1080 °C, the roasting temperature of pyrolusite was 775 °C, and the roasting time was 2 h, the maximum manganese reduction efficiency, nearly 100 %, could be obtained. The results of the manganese reduction efficiency of the actual experiments were close to those of the fitting model by the verification experiments, indicating that the optimum solution had a relatively high reliability.

(4) The fluidized roasting coupling technology is generally applicable to the extraction of various low-grade pyrolusite and it is promising to be utilized widely in manganese industry due to its high efficiency, good availability, and low cost.

Acknowledgements

This work was financially supported by the National Natural Science Foundation of China (NO. 21176026), the National High Technology Research and Development Program (863 program) of China (NO. 2012AA062401), and the National Key Technology R&D Program of China (NO. 2012BAB14B05).

References

- [1] F. Pagnanelli, M. Garavini, F. Vegliò, L. Toro, *Hydrometallurgy*, 71 (3–4) (2004) 319-27.
- [2] H. Su, Y. Wen, F. Wang, Y. Sun, Z. Tong, *Hydrometallurgy*, 93 (3–4) (2008) 136-9.
- [3] H. Su, H. Liu, F. Wang, X. L., Y. Wen, *Chinese Journal of Chemical Engineering*, 18 (5) (2010) 730-5.
- [4] R.N. Sahoo, P.K. Naik, S.C. Das, *Hydrometallurgy*, 62 (3) (2001) 157-63.
- [5] J.M.M. Paixdo, J.C. Amaral, L.E. Memória, L.R. Freitas, *Hydrometallurgy*, 39 (1–3) (1995) 215-22.
- [6] T.J.W. De Bruijn, T.H. Soerawidjaja, W.A. De Jongt, P.J. Van Den Berg, *Chemical Engineering Science*, 35 (7) (1980) 1591-9.
- [7] A. Jerez, M.A. Alario, *Thermochimica Acta*, 58 (3) (1982) 333-9.
- [8] Z. Cheng, G. Zhu, Y. Zhao, *Hydrometallurgy*, 96 (1–2) (2009) 176-9.
- [9] J.J. Song, G.C. Zhu, P. Zhang, Y.N. Zhao, *Acta Metallurgica Sinica-English Letters*, 23 (3) (2010) 223-9.
- [10] A.G. Kholmogorov, A.M. Zhyzhaev, U.S. Kononov, G.A. Moiseeva, G.L. Pashkov, *Hydrometallurgy*, 56 (1) (2000) 1-11.
- [11] Y. L., *Minerals Engineering*, 17 (9–10) (2004) 1053-6.
- [12] H.-Z. Long, L.-Y. Chai, W.-Q. Qin, *Transactions of Nonferrous Metals Society of China*, 20 (5) (2010) 897-902.
- [13] T.A. Lasheen, M.N. El Hazek, A.S. Helal, *Hydrometallurgy*, 98 (3–4) (2009) 314-7.
- [14] F.W.Y. Momade, Z.G. Momade, *Hydrometallurgy*, 51 (1) (1999) 103-13.
- [15] F.W.Y. Momade, Z.G. Momade, *Hydrometallurgy*, 54 (1) (1999) 25-39.
- [16] D. Hariprasad, B. Dash, M.K. Ghosh, S. Anand, *Minerals Engineering*, 20 (14) (2007) 1293-5.
- [17] X. Tian, X. Wen, C. Yang, Y. Liang, Z. Pi, Y. Wang, *Hydrometallurgy*, 100 (3–4) (2010) 157-60.
- [18] Z. Jianhua, L. Hongyu, T. Xike, W. Longyan, Y. Chao, P. Zhenbang, *Journal of China University of Geosciences*, 18 (2) (2007) 163-76.
- [19] M.S. Bafghi, A. Zakeri, Z. Ghasemi, M. Adeli, *Hydrometallurgy*, 90 (2–4) (2008) 207-12.
- [20] S.C. Das, P.K. Sahoo, P.K. Rao, *Hydrometallurgy*, 8 (1) (1982) 35-47.
- [21] M.N. El Hazek, T.A. Lasheen, A.S. Helal, *Hydrometallurgy*, 84 (3–4) (2006) 187-91.
- [22] S.-H. Do, B. Batchelor, H.-K. Lee, S.-H. Kong, *Chemosphere*, 75 (1) (2009) 8-12.
- [23] A.A. Nayl, I.M. Ismail, H.F. Aly, *International Journal of Mineral Processing*, 100 (3–4) (2011) 116-23.
- [24] D. Grimanelis, P. Neou-Syngouna, H. Vazarlis, *Hydrometallurgy*, 31 (1–2) (1992) 139-46.
- [25] P.K. Naik, L.B. Sukla, S.C. Das, *Hydrometallurgy*, 54 (2–3) (2000) 217-28.
- [26] W.-Y. Sun, S.-L. Ding, S.-S. Zeng, S.-J. Su, W.-J. Jiang, *Journal of Hazardous Materials*, 192 (1) (2011) 124-30.
- [27] S. Ma, S. Liu, *Hunan Nonferrous Metals*, 14 (4) (1998) 21-4.